A Theory of the Anti-Coronae

H. C. VAN DE HULST

*Astronomical Observatory, Utrecht, Holland**

(Received October 14, 1946)

The anti-coronae, or luminous rings around the anti-solar point, are explained as a peculiar diffraction phenomenon in small water drops. The optical and the electromagnetic theories give results in agreement with each other and with the observations. The most important features are those which relate to the polarization.

THE diffraction coronae, or colored rings, which surround the sun or moon, when covered by a thin veil of cloud, are well known. A similar phenomenon can occasionally be observed in the opposite direction. A person standing on a high point observes his shadow projected on low clouds or on a layer of mist. He observes a gradual increase of the intensity of reflected light towards the shadow's head and, if conditions are favorable, some colored rings appear around the head. We shall call this phenomenon the anti-corona.[1] It is often seen in the mist on mountain tops and occasionally in lower country, when the sun is near the horizon. An air-pilot related that he saw the anti-corona around the shadow of his plane on the clouds nearly every day. According to the position of the observer, the center of the rings shifts from the shadow of the head of the plane to the shadow of its tail. Once or twice the anti-corona has been studied in laboratory experiments.

A satisfactory explanation has not so far been available. The old explanation by which the anti-corona is ascribed to common diffraction of light somehow reflected around the foremost drops of the cloud, does not appear to be sound. The more recent view is that these peculiar fluctuations in the intensity of nearly backward scattered light are already present in the scattering diagram of one single drop. Thus far, however, a more specific theory explaining the differences between the common coronae and the anti-coronae, has not been given.

For a general investigation of the scattering of light by spherical particles, we refer to a former publication,[2] which gives an extensive treatment of dielectrical and absorbing particles on the basis of Mie's electromagnetical theory. Data from other authors are compiled, various limiting cases are discussed and numerical results are given. The present problem deals with the limiting case of very large particles, where the scattering approaches the classical theories of geometrical optics and of optical interference. We shall first derive the results from the optical theory and then from the rigorous electromagnetical formulae.

OPTICAL THEORY

The intensity of light scattered by a sphere which is large in comparison with the wavelength can be computed by means of the laws of geometrical optics. The additional scattering by diffraction around the sphere is irrelevant for the present subject. The resulting formula is (T. 5, 14)

$$2\pi I_{1,2}(\theta) = \sum \epsilon_{1,2}^2 |a|^2. \tag{1}$$

Here I is the emergent flux per unit solid angle, divided by the incident flux on the whole sphere; θ is the angle between the scattered and proceeding rays; finally the subscripts 1, 2 refer to the components the electric vectors of which are perpendicular and parallel, respectively, to the plane through the incident and scattered rays.

The intensities given by Eq. (1) consist of sums that have to be extended over all different light paths along which rays can be reflected, or refracted, into the direction θ. One light path can be specified by the parameters τ and p

---

[1] The frequent use of the common term "glory" (cf. Webster) was considered unsuitable in an article of this kind.

[2] H. C. van de Hulst, "Optics of spherical particles," Thesis Utrecht, 1946; also published in Rech. Astr. de l'Observatoire d'Utrecht, 11, Part I. Formulae from this work will be quoted as (T. 5, 14) etc.

which are, respectively, the angle between the incident ray and the surface of the sphere, and the number of internal reflections added to 1. The case $p=0$ means external reflection. For a given light path, $\epsilon_{1,2}$ (T. 5, 13) denotes the decrease of the amplitude caused by the partial reflection and refraction on account of Fresnel's theory. Furthermore $|a|^2$ accounts for the decrease in intensity caused by the geometrical divergence of the rays; the value of $|a|$ is (T. 5, 15):

$$|a| = \left| \frac{\sin \tau \cos \tau}{\sin \theta} \frac{d\tau}{d\theta} \right|^{\frac{1}{2}}. \qquad (2)$$

It has been observed long ago that the intensity given by (1) and (2) would become ∞ for a light path for which

$$d\theta/d\tau = 0. \qquad (3)$$

This condition defines the *rainbows*. The two main rainbows lie near:

$$p=2, \quad \tau=31°, \quad \theta=138°, \quad \pi-\theta=42°;$$
$$p=3, \quad \tau=18°, \quad \theta=129°, \quad \pi-\theta=51°.$$

A strict infinity does not occur if interference is taken into account. The rays defined by (3) and the adjacent rays with equal p but with slightly different τ form a cubic wave front and a classical calculation[3] yields the correct intensity curve for the rainbows and supernumerary bows.

A second case in which the expression (2) diverges occurs when

$$\sin \theta = 0, \text{ while } \sin 2\tau \neq 0. \qquad (4)$$

No attention has been paid to this case, though it is quite similar to the case of the rainbow. Again, the divergence can be removed by taking into account the interference with the adjacent rays; a determinate intensity distribution will then result.

Condition (4) implies the cases $\theta=0$ and $\theta=\pi$. All peculiarities in the intensity distribution near $\theta=0$ are blended by the much stronger coronae caused by the diffraction of light around the sphere. Near $\theta=\pi$, however, a peculiar phenomenon may be expected. Indeed, as we shall see, the observed anti-coronae are explained in this way.

---

[3] Airy's theory. See any textbook on meteorological optics.
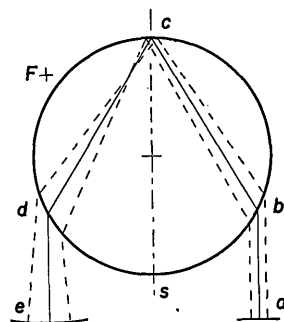

FIG. 1. Origin of toroidal wave front.

Figure 1 shows the simplest case of a light ray, *abcde*, satisfying the conditions required. Two adjacent rays, which emerge under slightly different angles, are also drawn. The linear front of the incident plane wave transforms into the circular front of the emergent wave, which has a virtual focus at F. However, still other rays must be taken into account. The whole figure must be rotated around the axis cs, and all the outgoing rays, thus defined, will interfere with each other. They define a *toroidal wave front* which seems to emerge from the focal circle described by F. We now have to calculate by means of Huygens' principle the interference pattern corresponding to this particular wave front.

The most interesting feature of the present problem is that the two directions of polarization cannot be treated separately. Let the incident wave be plane polarized with its electrical vector vibrating in the plane of Fig. 1. Then, for the rays drawn, it possesses a parallel vibration and emerges with an amplitude containing the factor ϵ_2. In the perpendicular plane, however, the same wave appears as a perpendicularly vibrating wave so that it is transmitted with an amplitude proportional to ϵ_1. Both transmitted waves are *still* vibrating in equal directions and are capable of interference. It is thus seen that the interference of rays in different azimuthal planes *simulates* an interference of rays with different directions of polarization.

Figure 2 explains the symbols we shall use in our analysis. The circle represents the focal circle from which the toroidal wave seems to emerge; let its radius be r'. We will compute the intensity radiated in a direction which makes a small angle γ with the axis and the projection of which on the plane of Fig. 2 is directed toward
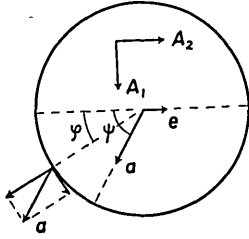
Fig. 2. Decomposition of light vectors.

the right, as shown by the arrow e. The consistent notations for the components of the light vector A of the emergent wave which vibrate parallel to and perpendicularly to the plane through the axis and e, are A_2 and A_1, respectively.

Let the incident light first be linearly polarized in a direction a making an angle ψ with the fixed direction mentioned. The light emerging from an arbitrary point of the focal circle, as specified by the angle φ, consists of two components which in the incident beam have the amplitudes $\cos(\psi - \varphi)$ in the outward radial direction and $\sin(\psi - \varphi)$ in the counterclockwise tangential direction. The amplitudes with which these components emerge are:

$$\text{radial: } C_2 \cos(\psi - \varphi) \qquad \text{tangential: } C_1 \sin(\psi - \varphi) \tag{5}$$

where the constants C_1 and C_2 are proportional to ϵ_1 and ϵ_2, respectively. To derive the amplitude vectors of the total emergent light wave, we must decompose the vector (5) into components with directions parallel to A_1 and A_2. These are:

$$a_1(\varphi) = (C_1 \cos^2 \varphi + C_2 \sin^2 \varphi) \sin \psi - (C_1 - C_2) \sin \varphi \cos \varphi \cos \psi,$$
$$a_2(\varphi) = (C_1 - C_2) \sin \varphi \cos \varphi \sin \psi - (C_1 \sin^2 \varphi + C_2 \cos^2 \varphi) \cos \psi. \tag{6}$$

Writing $r' \sin \gamma = r'\gamma = u$, we now find the total amplitudes of the emergent light to be

$$A_{1,2} = \frac{1}{2\pi} \int_0^{2\pi} e^{-iu \cos \varphi} a_{1,2}(\varphi) d\varphi. \tag{7}$$

The definite integrals needed to reduce this expression,

$$\frac{1}{2\pi} \int_0^{2\pi} e^{-iu \cos \varphi} \cos^2 \varphi d\varphi = \tfrac{1}{2}\{J_0(u) - J_2(u)\},$$

$$\frac{1}{2\pi} \int_0^{2\pi} e^{-iu \cos \varphi} \sin^2 \varphi d\varphi = \tfrac{1}{2}\{J_0(u) + J_2(u)\},$$

$$\frac{1}{2\pi} \int_0^{2\pi} e^{-iu \cos \varphi} \sin \varphi \cos \varphi d\varphi = 0,$$

are related to Sommerfeld's integral defining the Bessel functions.

Incident natural light can be considered as a superposition of non-coherent linearly polarized waves with randomly distributed directions of vibration. Averaging, therefore, the intensities in respect to ψ, we find a factor $\langle \sin^2 \psi \rangle_{Av} = \langle \cos^2 \psi \rangle_{Av} = \tfrac{1}{2}$ both in A_1^2 and in A_2^2. With omission of the factor $\tfrac{1}{8}$, the final intensities are:

$$I_1 = [C_1\{J_0(u) - J_2(u)\} + C_2\{J_0(u) + J_2(u)\}]^2$$
$$I_2 = [C_2\{J_0(u) - J_2(u)\} + C_1\{J_0(u) + J_2(u)\}]^2 \tag{8}$$

and in both directions of polarization together:

$$I = 2(C_1 + C_2)^2 J_0^2(u) + 2(C_1 - C_2)^2 J_2^2(u).$$

These formulae show the full implications of the interference effect described. If no interference between rays in different azimuthal planes took place, the intensities $I_{1,2}$ would contain only the coefficients $C_{1,2}$ with the *same* index. This is the case for the rainbow; it holds also for large angles in the present theory: with increasing distance from the center of the interference pattern the factor

$J_0(u) + J_2(u)$ decreases rapidly, like $u^{-\frac{3}{2}}$, leaving

$$J_0(u) - J_2(u) = (8/\pi u)^{\frac{1}{2}} \cos\,(u - \pi/4)$$

with the same index coefficient as the predominant term.[4] For small u, however, the terms of (8) are of the same order of magnitude; this region will be discussed in the last section.

ELECTROMAGNETICAL THEORY

The general expression for the intensity distribution of light scattered by a homogeneous sphere was first derived by Mie in 1908.[5] The resulting formulae in a somewhat changed notation (T. 2, 12) are:

$$\pi I_{1,2}(\theta) = \frac{1}{2x^2} |\textstyle\sum_{1,2}|^2, \tag{9}$$

where

$$\sum_1 = \sum_{n=1}^{\infty} \frac{2n+1}{n(n+1)} \{a_n \pi_n(v) + b_n \tau_n(v)\},$$

$$\tag{10}$$

$$\sum_2 = \sum_{n=1}^{\infty} \frac{2n+1}{n(n+1)} \{b_n \pi_n(v) + a_n \tau_n(v)\}.$$

By x we denote the ratio $2\pi r/\lambda$, the circumference of the sphere in terms of the wave-length. The coefficients a_n and b_n refer to the electric and magnetic 2^n-poles, respectively; they are complex functions (T. 2, 7) of x and of the refractive index, m. Finally, the formula contains the spherical harmonics (T. 2, 10):

$$\pi_n(v) = \frac{1}{\sin\theta} P_n^1(v) \quad \text{and} \quad \tau_n(v) = \frac{d}{d\theta} P_n^1(v),$$

where $v = \cos\theta$.

Anti-coronae in visible light are observed on clouds consisting of drops with diameters of the order of 25μ, which corresponds to a value for x of about 150. For such a large value of x the evaluation of expressions (9) is impracticable so that we have to use their asymptotic forms. We denote the small angle $\pi - \theta$ by γ. The spherical harmonics have then the asymptotic forms (T. 5, 5):

$$\pi_n(v) = (-1)^{n-1} \frac{n(n+1)}{2} \{J_0(z) + J_2(z)\},$$

$$\tag{11}$$

$$\tau_n(v) = (-1)^n \frac{n(n+1)}{2} \{J_0(z) - J_2(z)\},$$

where we have written $z = n\gamma$.

As was stated by Debye, the terms of (10) are of comparable size up to $n = x$ and decrease rapidly as soon as n exceeds x. Most of these complex terms will nearly cancel each other. Only when the terms of the order

$$N-3,\ N-2,\ N-1,\ N,\ N+1,\ N+2,\ N+3,\ \cdots$$

have nearly equal phases, does an appreciable total amplitude result. In particular, the amplitudes of the nearly backward scattered light will be determined by the terms near the order N for which the sums

$$c_1 = \sum_n (2n+1)(-1)^n b_n, \quad c_2 = \sum_n (2n+1)(-1)^{n-1} a_n, \tag{12}$$

consist of terms with stationary phases. Neglecting the effect of the further terms, we find from

---

[4] By comparing this asymptotic behavior of (8) with Eq. (1) the relative coefficients may be expressed in absolute units.
[5] G. Mie, Ann. d. Physik **25**, 377 (1908).

(10) and (11) the total amplitudes

$$\sum\nolimits_1 = \tfrac{1}{2}c_2\{J_0(u)+J_2(u)\}+\tfrac{1}{2}c_1\{J_0(u)-J_2(u)\},$$
$$-\sum\nolimits_2 = \tfrac{1}{2}c_1\{J_0(u)+J_2(u)\}+\tfrac{1}{2}c_2\{J_0(u)-J_2(u)\},$$

(13)

where u is written for $N\gamma$. These formulae, when substituted into (9), agree with the optically derived formula (8). Only the values of c_1, c_2 and N have still to be calculated.

Before we proceed, attention may be drawn to the following point. In Debye's asymptotic formulae (T. 5, 8) the coefficients a_n and b_n refer to *one* direction of polarization. Yet they appear simultaneously in the amplitudes for *each* direction of polarization. This apparent paradox can now be completely explained. In the asymptotic form the term with the different index drops out for most directions because $\pi_n(v)$ has a smaller order of magnitude than $\tau_n(v)$. Only near the forward or backward directions the mixture of both terms remains and can be fully explained on the basis of Huygens' principle, as was shown in the preceding section.

The final step consists of the determination of N, c_1, and c_2 from (12). We may evaluate them either analytically or numerically.

a. By the analytical procedure we can formally demonstrate the complete equivalence of the optically and electromagnetically derived formulae for drops which are very large in comparison with the wave-length. Similar proofs have been given for the special case of the rainbow[6] and for the general case[7] in which expression (2) has no discontinuity. The modification for the present special case would present no difficulties. In each of the three cases we start by replacing the coefficients a_n and b_n by their asymptotic forms for very large order, according to Debye. Different expressions are needed for $n<x$ and for $n>x$, as can be visualized by means of the "localization principle," which assigns the terms of the order n to rays passing the center at a distance $n\lambda/2\pi$. Terms with $n>x$ correspond to rays passing along the sphere and give a vanishing contribution. Terms with $n<x$ correspond to rays hitting the sur-

face under an angle $\tau = \arc\cos(n/x)$. Further, the asymptotic form for each term can be decomposed into subterms corresponding to different numbers of internal reflections, each of them with the proper coefficients ϵ_1, or ϵ_2. It appears that b_n refers to the perpendicularly vibrating wave (index 1) and a_n refers to the parallel wave (index 2). Finally, the subterms have a stationary phase for the order N which corresponds exactly with the location of the classical light paths. The sum of the terms of orders near N can be approximated by a Fresnel integral or, in the case of the rainbow, by an Airy integral. The resulting intensities, polarizations and phases agree with the optically derived results. For the anti-corona we would conclude that $N\lambda/2\pi$ is equal to the radius r' of the focal circle and that c_1 and c_2 are, like C_1 and C_2, proportional to ϵ_1 and ϵ_2.

b. The analytical derivation of N, c_1, and c_2 of which we gave an outline holds for the general case defined by Eqs. (4). However, our assumption that the actual anti-coronae are caused by light rays satisfying these conditions is not correct: a light path as illustrated in Fig. 1 does not exist for a waterdrop. When we pass from central rays to edge rays the deviation γ of the ray with a single internal reflection increases from 0° to 42° (rainbow) and decreases again to the final value of 14°. The value $\gamma=0°$ is not again reached. This would seem to invalidate our explanation. On the other hand, it must be pointed out that centrally incident rays, though they give $\gamma=0$, give a perfectly smooth intensity distribution since the discontinuity of expression (2) is removed by the fact that also $\cos\tau=0$.[8] Further, a rough computation shows that the more complicated light paths give rise to anti-coronae that are too weak to be observed, just as is the case for rainbows caused by more than two internal reflections.

The following simple solution is suggested as the most probable: though x can be as large as

[6] Balth. van der Pol and H. Bremmer, Phil. Mag. **24**, 141 and 825 (1937). Further articles on an analogous problem, *ibid.* **25**, 817 and **27**, 261.

[7] The outline given here follows the treatment by H. C. van de Hulst, reference 2, Chapter V.

[8] The explanation by B. Ray, Proc. Ind. Ass. for the Cultivation of Science **8** (1923), is not correct, for this reason.

200, the actual drops are still small enough to give strong deviations from the results for the optical case, $x \to \infty$. The following considerations tend to support this explanation. A light path as shown by Fig. 1 exists for refractive indices between 2 and $\sqrt{2}$. The angles of incidence required are given in Table I. It is obvious that $m = 1.33$ just fails to satisfy the conditions, if the optical theory is to be rigorously valid. For a finite value of x, however, the change at $m = 1.41$ will not be so abrupt. From the values of $\cos \tau$, which is equal to N/x, we see that the anti-corona is caused by rays near the edge of the droplet. We therefore infer that also for $m = 1.33$ the *radius of the focal ring is nearly equal to the radius of the droplet.*

Furthermore, we know that Debye's semi-convergent formulae for the cylindric functions, on which the proof of the equivalence between the optical and the electromagnetical results was based, are *not* valid for n near x. E.g., for $x = 150$ they are useless for the terms ranging from about $n = 144$ to 156.[9] This makes the optical theory for the anti-coronae completely unreliable for spheres with $x = 150$ and $m = 1.6$ to 1.41. Consequently, it is probable that drops of this size and of refractive index 1.33 still give a strong anti-corona.

The values of c_1 and c_2 cannot now be derived from the analytical theory. Instead, we should compute the values of a_n and b_n from their rigorous definitions and add the sums (12) *numerically*. The optical considerations only predict a stationary phase of the terms near $n = x$. We have not made such a computation and, accordingly, we cannot give a theoretical prediction about the ratio of c_1 to c_2.

TABLE I. Rays that would give rise to anti-coronae if the refractive index were m.

m	τ	$\cos \tau$
2.0	90°	0
1.9	54°	0.59
1.8	38°	0.78
1.7	26°	0.90
1.6	16°	0.96
1.5	7°	0.99
1.41	0°	1.00
1.33	—	—

[9] See Jahnke-Emde, *Tables of Functions* (B. G. Teubner, Leipzig, 1933 edition), especially Fig. 105.
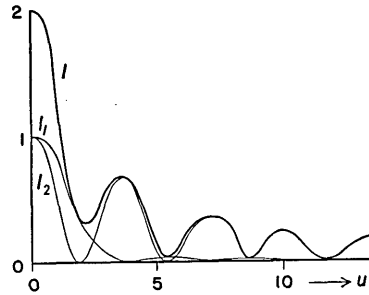

FIG. 3. Intensity distribution of the anti-coronae in both directions of polarization, in case $C_1 = 0$.

COMPARISON WITH THE OBSERVATIONS

For any given ratio of C_1 to C_2 the relative intensities in both directions of polarization can be readily evaluated from (8). The results for a few cases are:

1. $C_1 = C_2$. The anti-corona is wholly unpolarized. The central field is very luminous and dark rings appear at $u = 2.5$, 5.6, 8.7, 11.8, $\cdots$.

2. $C_1 = -C_2$. The anti-corona is again unpolarized. The anti-solar point is dark and is surrounded by a luminous ring at $u = 3.1$. Dark rings are situated at $u = 5.2$, 8.5, 11.6, $\cdots$.

3. $C_1 = 0$. The intensities for this case are shown by Fig. 3. In the central field the "alien" polarization, index 1, is slightly preponderant except at the anti-solar point itself. At $u = 2.3$ we find a fairly dark ring in which the polarization changes its sign. The bright ring at $u = 3.5$ and all further rings are nearly completely polarized in the "proper" direction, index 2. They are separated by dark rings at $u = 5.4$, 8.6, 11.7, $\cdots$.

We shall now compare these predictions with the available *observations*. Data concerning anti-coronae on natural clouds have been collected by Pernter-Exner.[10] Measurements on artificial mist, together with qualitative observations of the polarization, have been published by Mierdel.[11] These data, though not obtained with modern observational technique, suffice to give some checks on the theory and a preliminary determination of C_1/C_2.

The anti-coronae show distinct *differences from common coronae*, all of which can be explained on the basis of the present theory. (a) One feature is

[10] Pernter-Exner, *Meteorologische Optik* (W. Braumüller, Wien, 1910), p. 413 ff.
[11] F. Mierdel, Beiträge z. Physik d. freien Atmosphäre 8, 95 (1919).

TABLE II. Ratios of the radii of the dark rings.

Observer	Light	Cloud	γ_1/γ_2	γ_3/γ_2
Mierdel	white	artificial	0.34 ± 0.05	1.66 ± 0.03
	red	artificial	—	1.68 ± 0.04
	photographic	artificial	—	1.59
Average of several observations	white	natural	0.46 ± 0.05	1.67 ± 0.06
Wegener	photographic	natural	0.41	(1.74)
Theory	$C_1=0$		0.43	1.60
	$C_1/C_2=-0.25$		0.35	1.61

their variability. It is obvious that the interference of rays which are refracted by opposite sides of a waterdrop will be much more sensitive to slight deformations of the droplets than are the rainbows in which only adjacent rays interfere, or the common coronae in which non-refracted rays interfere. (b) The outer rings of anti-coronae are much more pronounced than are the outer rings of common coronae. On one occasion as much as 5 minima could be observed. The explanation is that the intensity in the anti-coronae decreases proportionally to γ^{-1}, whereas common coronae follow a θ^{-2}-law. (c) A final striking feature is the haziness of the first dark ring (which for normal sunlight is observed as the first red ring). Mierdel even calls it a slight depression separating the inner and outer parts of the central field. This haziness can be understood if the intensity distribution of Fig. 3, is approximately correct. A further increase of the first bright ring is obtained if we approach case 2, where C_1 and C_2 have opposite signs. Estimating from Mierdel's description that

$$0.30 < \frac{\text{brightness of first ring}}{\text{brightness of central field}} < 0.80,$$

we find the value of either C_2/C_1 or C_1/C_2 to lie between 0 and -0.25.

Further information is obtained from Mierdel's observations of the *polarization*. From the fact that the picture rotates with the analyzing nicol we infer circular symmetry to exist so that the glass plates in Mierdel's experiment cannot have had a serious effect. The complementary colors of the central field and the rings indicate different planes of polarization, in agreement with Fig. 3. The preponderant polarization in all bright rings is the one in which the electric vector vibrates

in the radial direction. This shows that $C_2>C_1$, disregarding signs. Still, the tangential component is also visible. Estimating its intensity to exceed 4 percent of the total intensity of the rings, we find $C_1^2/C_2^2>0.04$. Together with the former data this indicates that C_1/C_2 must be about $-\frac{1}{4}$ or $-\frac{1}{5}$. This estimate is based on laboratory data; no observations of the polarization of natural anti-coronae seem to have been published.[12]

Finally we use the *radii* of the rings. As is true for common coronae, the radii of the rings are inversely proportional to the sizes of the droplets. However, it was noticed long ago that the rings of anti-coronae do not give consistent sizes when interpreted with the older theory. Let us denote the radii of the dark rings by γ_1, γ_2, γ_3, etc. For $C_1=0$, the present theory gives

$$\gamma_1:\gamma_2:\gamma_3:\gamma_4=2.3:5.4:8.6:11.7$$
$$=0.43:1.00:1.60:2.17.$$

For other values of C_1/C_2 the ratios are not very different. Table II shows the observed and computed ratios.

The agreement between theory and observations is as good as can be expected. No correction has been applied for the size of the sun and it was assumed that the edges of the red rings, which were measured by the observers, indicate the positions of the *dark* rings in the monochromatic picture for yellow light.[13] This introduces a considerable uncertainty but the ratio $\theta_2/\theta_1=1.80$, valid for the common diffraction coronae, differs strongly enough from the tabulated values to indicate again that this theory does not apply to the anti-corona.

On the basis of the present theory, measurements of the various dark rings give consistent sizes for the droplets. From the average diameters, which are about $2\gamma_1=1°\,30'$, $2\gamma_2=3°\,50'$, $2\gamma_3=6°\,30'$, we find 0.027 mm for the average diameter of the water drops in the clouds on which anti-coronae have been observed.

---

[12] Dr. O. Struve has related to me that he observed an anti-corona through a nicol prism on a transatlantic flight, Sept. 15, 1946. It was strongly polarized and the dark and bright features rotated when the nicol was rotated. No radii or intensities were however estimated.

[13] Early experiments by Fraunhofer indicated that this rule was correct for the first three rings of common coronae. The "wave-length of white light" is 0.57μ. See Pernter-Exner, p. 460.